

## Experimental and numerical prediction of the weakened zone of a ceramic bonded to a metal

Bouchra Zaoui\*, Mohammed Baghdadi, Belaid Mechab,  
Boualem Serier and Mohammed Belhouari

*Department Faculty of Technology, LMPM, Mechanical Engineering, University of Sidi Bel Abbes, Algeria*

*(Received February 26, 2019, Revised January 2, 2020, Accepted January 27, 2020)*

**Abstract.** In this study, a three-dimensional Finite Element Model has been developed to estimate the size of the weakened zone in a bi-material a ceramic bonded to metal. The calculations results were compared to those obtained using Scanning Electron Microscope (SEM). In the case of elastic-plastic behaviour of the structure, it has been shown that the simulation results are coherent with the experimental findings. This indicates that Finite Element modeling allows an accurate prediction and estimation of the weakening effect of residual stresses on the bonding interface of Alumina. The obtained results show us that the three-dimensional numerical simulation used by the Finite Element Method, allows a good prediction of the weakened zone extent of a ceramic, which is bonded with a metal.

**Keywords:** bi-materials (ceramic/metal); damage; stress intensity factor; J integral; prediction

---

### 1. Introduction

Advanced bi-materials consist of two or more materials with different mechanical, physical and chemical properties. The interface between these different materials has a significant influence on the strength and toughness of bonded materials (Boutabout *et al.* 2009, Hu *et al.* 2017).

Bi-material systems may be found in numerous engineering devices, structures, and applications. other more common applications includes laminated beams, coated systems for mechanical devices, and layered composites for main structural applications or micro-electronic chips (Liu *et al.* 2017).

Several theoretical and experimental methods have been explained by researchers in the past to investigate mechanism of crack propagation through different materials (Sih and Rice 1965, England 1965, Erdogan and Biricikoglu 1973, Rice 1988, Hutchinson and Suo 1991).

In a bi-material fractured test specimen, the stress intensity factors are influenced by the mechanical properties of each material as well as the specimen geometry (Xu *et al.* 2008, Itou 2007, Zhang and Qiao 2017).

Datta *et al.* (2018) developed an analytical model based on the Rice's path independent J-Integral. The analytical model results have shown a good coherence with the experimental findings.

---

\*Corresponding author, Ph.D., E-mail: [bmechab@yahoo.fr](mailto:bmechab@yahoo.fr)

Ouinan *et al.* (2008) studied the effect of the difference between the elastic modulus of the metal and ceramic on the direction, and the rate of crack propagation.

In another study on the influence of weak interface between particles and matrix on mechanical properties of metal matrix - ceramic reinforced composites with poor interfacial bond Jarzabek (2018) showed, that after tensile test on these composites the Young's modulus takes values of  $67 \pm 8$  GPa and the ultimate tensile strength  $230 \pm 15$  MPa. These authors assume that these values result from the low resistance of the interface. These authors have developed a numerical model, in terms of analysis of the mechanical behavior of the interface, to better understand this hypothesis. They conclude that this model confirms the experimental results. To this end, a representative volume element has been created and modeled by the Finite elements Method with cohesive zone elements. This modeling leads to Young's modulus values of 119 GPa to 126 GPa.

The same author Jarzabek *et al.* (2016) developed an experimental approach, allowing the characterization of the mechanical resistance of the reinforcement-matrix interface of metal matrix composites reinforced by ceramic particles. These authors showed that the adhesion force between the reinforcing material and the matrix is higher as these particles are of large sizes.

In the present study, a three-dimensional Finite Element Model has been developed to estimate the size of the weakened zone in the bi-materials a ceramic bonded to a metal. The calculations results were compared to those obtained using Scanning Electron Microscope (SEM). In the case of elastic-plastic behaviour of the structure, it has been shown that the simulation results are coherent with the experimental findings. This indicates that Finite Element modeling allows an accurate prediction and estimation of the weakening effect of residual stresses on the bonding interface of Alumina.

## 2. Results and discussion

As explained earlier, the bonding process is performed at high temperature. As a result, internal residual stresses are generated during the cooling phase of the elaboration process, and they are situated near to the interface. As the metal cools down, it shrinks much more than ceramic, resulting in shear stresses at the interface between these two materials

$$\varepsilon_m = \alpha_m(T_0 - T) \quad \text{and} \quad \varepsilon_c = \alpha_c(T_0 - T) \quad (1)$$

m and c stands for metal and ceramic respectively.

$\alpha_m$  and  $\alpha_c$  are the thermal expansion coefficients of the metal and the ceramic respectively.

$(T-T_0)$  is the temperature difference between the bonding temperature and the room temperature.

Haussonne *et al.* (2005) showed that according to Eshelby analytical approach, these internal stresses depend on the difference between the thermal expansion coefficients of the ceramic, and the metal, and the difference between the temperatures values during the cooling phase, and on the modulus of elasticity and Poisson's coefficients of both materials

$$\sigma_R = \frac{(\alpha_m - \alpha_c)(T - T_0)}{\frac{1 + \nu_m}{2E_m} + \frac{1 - 2\nu_c}{E_c}} \quad (2)$$

The analysis of these residual stresses has been the subject of several studies. Beševic (2012)

presented experimental research, about the effect of residual stresses in the design of steel structures. He found that the effect of these stresses depend on their magnitude, orientation as well as their distribution. Hattali *et al.* (2009a) showed that residual stresses have the major role in the generation and propagation of cracks at the interface between metal and ceramics. In the case of bonding ceramic and metal by soldering, the authors Cazajus *et al.* (2012) have analyzed numerically the effect of the residual stresses on the quality of the soldering. They concluded that these stresses can significantly reduce the mechanical strength of end-use product obtained by metal-ceramic bonding. In another study, Charles *et al.* (2005), showed that residual stresses are generated in the weakened region which is the metal-ceramic interface, and that they are behind the initiation and creation of cracks in ceramics. Based on the hypothesis of the weakest bond, these authors have proposed a probabilistic model of cracking. Serier *et al.* (2011) have highlighted diffusion phenomena during metal-ceramic bonding and they explained the effect of residual stresses, on the mechanical strength of this bond. In this context, Ma *et al.* (2013) showed more light on the effect of thermal stresses, induced by the difference of properties between metals and ceramics, can lead to a failure at the interface. Hwang *et al.* (2015) explained that Selective Surface in Hybrid composites (FSS) have been developed to offer excellent specific mechanical and electromagnetic properties. Doitrand and Leguillon (2018) considered that in an industrial process, experimental measurements can be expensive and time consuming, so predictive modeling is highly needed. The present work focus on this issue. It aimed at predicting the damage size “h” of the ceramic (Alumina) bounded to metal (Silver) by employing a three-dimensional Finite Element model. The fracture energy will be calculated in term of stress intensity factors  $k$  (in the case of the elastic behaviour of the structure) and in term of the J integral (in the case of the elastic-plastic behaviour of the structure). The simulation results are compared to experimental findings obtained by scanning electron microscopy (SEM).

### 2.1 Experimental analysis of the weakened zone size of the ceramic

This is an experimental study about the extent of the weakened zone, of ceramic bonded to a solid metal at high temperatures. It concerns the mechanical strength of the interface and the fracture strength of ceramic.

For this purpose, polycrystalline alumina “SCT, “advanced technical ceramics” samples are used. The samples, obtained by solid state bonding carried at air (Fig. 2(a)), consists of two alumina cylinders (12 mm and 8 mm diameters and 3 mm thickness) which are both bonded to a silver (8 mm diameter, 0.5 mm thickness) under the action of a bonding pressure (P) and temperature (T), (Fig. 1). For this study, two assumptions were made, the two aims will be:

- The optimization of temperature (T): the time:  $t = 2\text{h}$  (is fixed), the temperature T: varies from  $500^{\circ}\text{C}$  to  $900^{\circ}\text{C}$  and the bonding pressure  $P = 6\text{ MPa}$  (Fig. 4).
- The optimization of time period of solid state bonding (t): the temperature  $T = 900^{\circ}\text{C}$  (is fixed), the time t: varies from 1h to 7h and the pressure  $P = 6\text{ MPa}$  (Fig. 8).

Then tested under uniaxial tension loading considering the real contact area between ceramic and metal (Figs. 2(a)-(b)), the loading rate is  $0.1\text{ mm/mn}$  (the speed of the test is  $0,1\text{ mm/mn}$ ). The analysis by scanning electron microscopy (SEM) shows that alumina is composed of very fine grains (see Fig. 3). An indirect tensile test known as a “push test” was used to characterize the mechanical strength of alumina-silver “Ag/Al<sub>2</sub>O<sub>3</sub>” assembly (Fig. 2(a)). This test, which directly subjects the interface to tension load F, does not require any clamping system it has a cylindrical

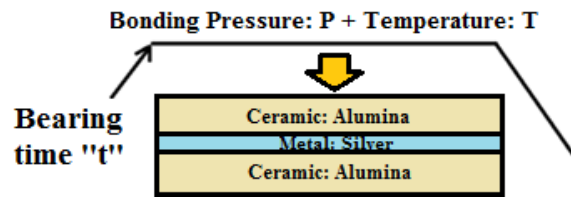


Fig. 1 Elaboration of ceramic-metal bond by solid state bonding

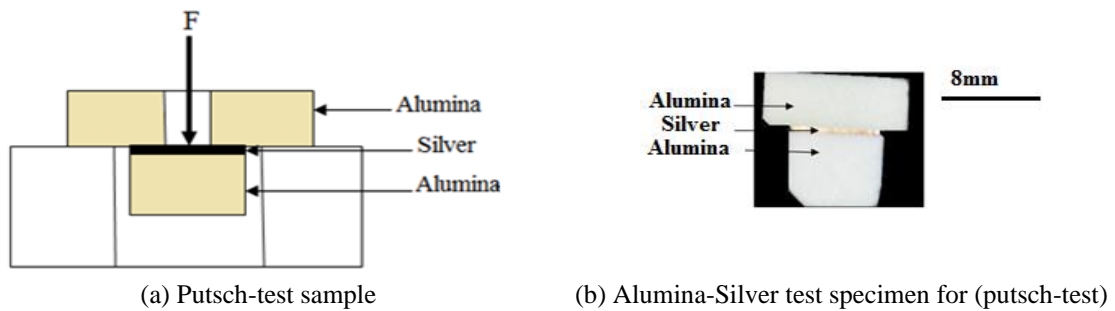


Fig. 2 Realization of Putsch test (characterization of the bi-material Alumina -silver interface)

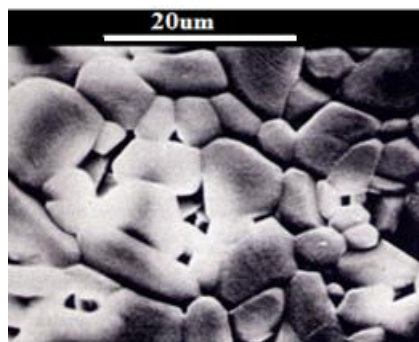


Fig. 3 Microstructure of SCT Alumina after a thermal attack of 10 h at 1500°C

specimen in the form of a pierced disc through which a punch comes to bear with an effort  $F$  on the metal. This test called, Putsch test, allows to solicted directly the interface as shown in Fig. 2(a). The bi-material  $Ag/Al_2O_3$  was chosen for this study, because of its many applications in electronics. Indeed, silver is the best conductor of electricity, presenting the best electrical conductivity ( $62.1 \cdot 10^6$  Siemens/m) and a very low electrical resistivity ( $10^{-8}$  Ohms.m) among all metals compared to copper. Alumina is the most very high performance ceramic material. It presents very interesting electrical properties (high resistivity, high dielectric constants, low dielectric loss factor, excellent dielectric properties in the case of direct currents or even high frequencies currents). The push test results are illustrated in Fig. 4, and they show that the tensile strength ( $\sigma_f$ ) of the ( $Ag/Al_2O_3$ ) is better when the bond is made at high temperatures, due to the creation of cohesive interfaces (Fig. 4). Fracture surface analysis using scanning electron microscopy (SEM) shows that the damage begins at the external boundary of the assembly and

Table 1 Characteristics of the alumina used

Alumina (SCT, advanced technical ceramics) AL <sub>2</sub> O <sub>3</sub>	
Composition % by weight	99.90%
Density (g/cm <sup>3</sup> )	3.95
Compressive strength at 20°C (MPa)	3000
Tensile strength at 20°C (MPa)	250
Bend Strength at 20°C (MPa)	320
Young's modulus (GPa)	320
Critical stress intensity factor (MPa.m <sup>1/2</sup> )	5.20
Poisson's ratio	0.27
Thermal expansion coefficient (°C <sup>-1</sup> ) at (20 to 1000)°C	7.50.10 <sup>-6</sup>
Maximum operating temperature (°C)	1660

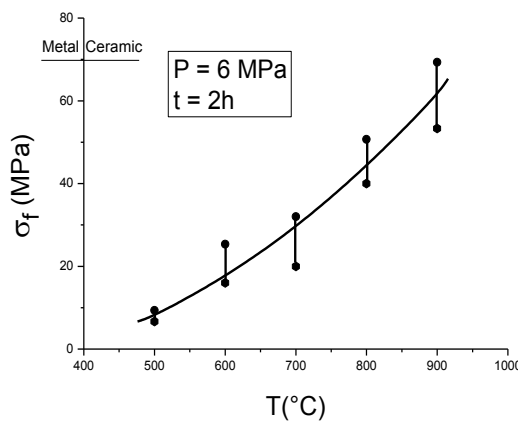


Fig. 4 Fracture tensile stress variation vs. elaboration temperature

then propagates deeply in the alumina body. The extent of this propagation is related to the bonding temperature and it becomes deeper when the temperature of the bonding process is close to the melting point of Silver (Figs. 5 and 6). Two types of fractures were observed: inter-granular fracture of small grains, and trans-granular fracture through large grains cleavage (see Fig. 6(b)). The failure occurs in the ceramics (Figs. 5 and 6(a)), that are near the interface, at stresses approximately four times lower than the tensile strength of the alumina, without any bonding to metal (see Fig. 4 and Table I). The zone size corresponding to this stress difference, was determined by scanning electron microscopy (see Fig. 5). It corresponds to a depth of 0.70 mm (see Fig. 5). In other terms, the latter corresponds to the extent of the residual stresses induced in alumina during the bonding process. Bonds developed at relatively low temperatures, result in poor mechanical resistance of the interface (see Fig. 4). In this case, the electron microscopy analysis shows that the failure initiates and propagates along the interface (adhesive failure) (Figs. 5 and 7). These figures clearly illustrate that the silver surface is partially covered by removed alumina grains (Figs. 7(a)-(b)). These experimental results show that the temperature at which alumina is bonded to silver is a key parameter for the mechanical strength of the metal-ceramic

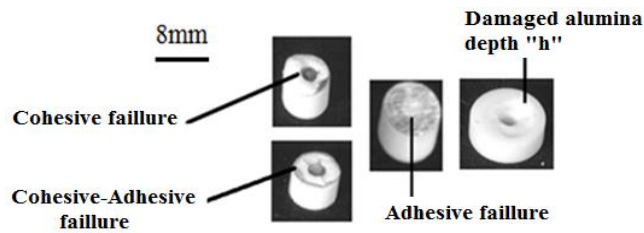
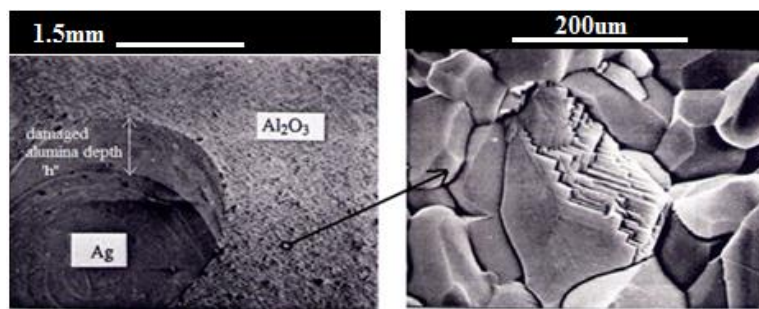
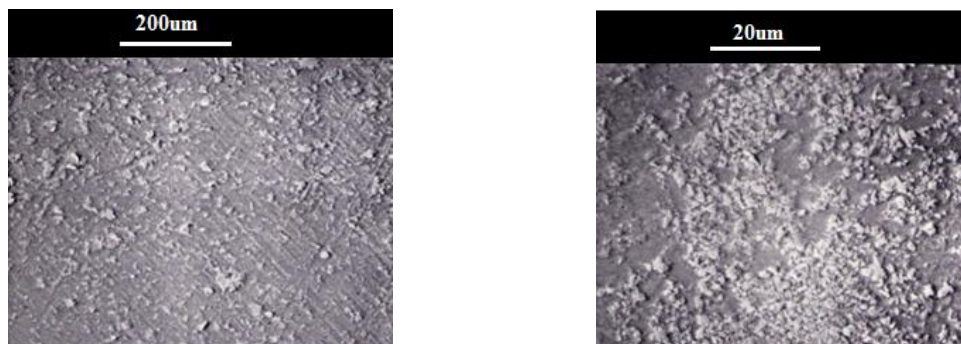


Fig. 5 Fracture surfaces of alumina-silver assemblies after pusch-test



(a) Damaged depth "h" (b) Observed failure mode  
 Fig. 6 Cohesive fracture of alumina in the Ag/Al<sub>2</sub>O<sub>3</sub> bond elaborated at 900°C



(a) Elaborated at 700°C during 2 h (b) Elaborated at 800°C during 2 h  
 Fig. 7 Adhesive fracture after the tensile test of the assembly Ag/Al<sub>2</sub>O<sub>3</sub>

interface. Indeed, high temperatures accelerate the diffusion of silver atoms and facilitate the migration process, into the alumina surface defects, leading to rigid and strong bonds. However, they generate high residual stresses, thus increasing the risk of a ceramic brittle fracture near to the interface at significantly lower stresses than its tensile failure limit. This behavior was observed during the bending tests of these assemblies (see Fig. 8). This figure clearly illustrates that the tensile strength ( $\sigma_t$ ) of the assembly, is about three times lower than the bending strength of non-bonded alumina (Table I). Through the analysis of the fracture surfaces, three types of damages, observed at 900°C, can be identified: adhesive, cohesive, and cohesive-adhesive type (see Fig. 8). Cohesive failure occurs at early times in alumina near the interface at significantly lower stresses

than the maximum tensile and bending limits of the non-bonded alumina. Sample analysis shows that the crack begins at the interface in the external boundary of the assembly body, then deflects towards the alumina, and propagates almost in parallel direction to the interface along the weakened zone.

In order to characterize this zone of ceramics which is in a high interaction with silver, an analysis of the resistance to cracking, using the indentation method, was performed. This technique is simple to apply and allows obtaining results similar to those obtained using conventional methods. The critical stress intensity factor was determined from the relationship of Liang *et al.* (1990)

$$K_{IC} = (H_v a^{1/2} / \alpha) \cdot (E\Phi / H_v)^{0.4} \cdot (C/a)^{c/18a-1.51} \quad (3)$$

Where ( $H_v$ ) is the Vickers hardness, ( $E$ ) the Young's modulus, ( $\Phi$ ) the stress factor equal to 3 for alumina, ( $c$ ) the size of the crack emanating from the diagonal print "a" (see Fig. 9) and  $\alpha$  is a non-dimensional constant which is a function of the Poisson's ratio ( $\nu$ )

$$\alpha = 14 \cdot \left[ 1 - 8 \left( \frac{8\nu - 0.5}{1 + \nu} \right)^4 \right] \quad (4)$$

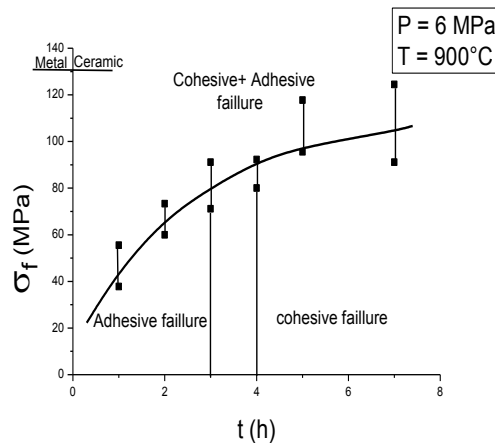


Fig. 8 Fracture tensile stress vs. bonding time

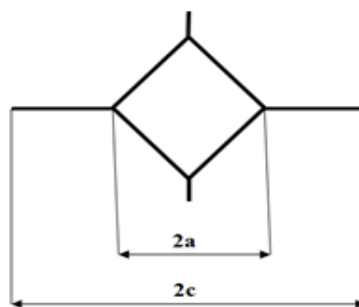


Fig. 9 Prints of indentation

Indentation imprints have been made on alumina which is bonded to silver under a loading, of 300 g for 15 secondes, higher than the critical cracking load, every 50  $\mu\text{m}$  from the interface (depth  $h$ ) to the “core” of the ceramic (see Fig. 10(a)). The cracks resulted from the imprint (Fig. 10(b)) propagate in parallel to the interface. Fig. 12 shows that the critical stress intensity factor of this alumina is affected at a depth of about 200  $\mu\text{m}$ . This is mainly due to the presence of residual stresses in the ceramics resulting from the difference in thermal expansion coefficients between silver and alumina. This decline in toughness explains the cohesive ruptures observed in alumina when the interfacial adhesion is good. Beyond this depth, the strength fracture is similar to that of a pure ceramic.

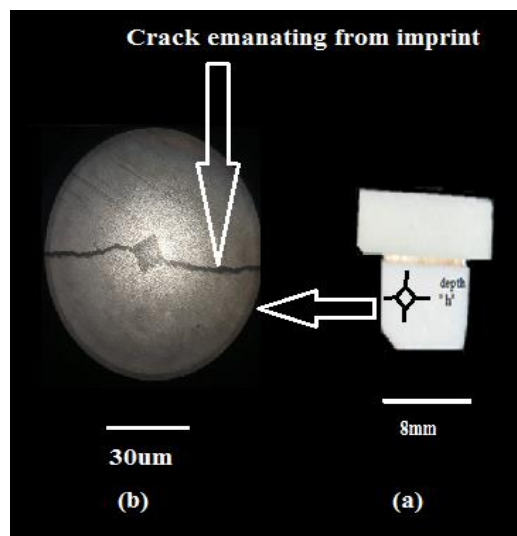


Fig. 10 Specimen for measuring of the toughness of alumina by indentation

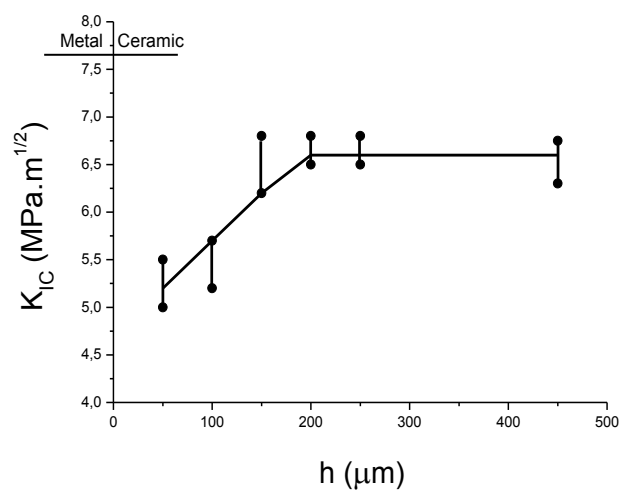


Fig. 11 Variation of the toughness measured with Vickers indentation vs. the distance to the interface at (900°C) during (4 h)



After the initiation of a crack by pure tensile load, the residual stresses relaxation contributes to its deviation towards the alumina far from the interface, leading to much more volume removal. This seems to explain the difference in the depth of the weakened zone measured by scanning electron microscopy and that determined by the indentation technique.

For the prediction of the weakened zone of silver bonded to alumina, a three-dimensional numerical analysis using the finite element method was carried out.

Bi-materials elaboration at high temperature, as in the case of ceramic-metal bond, weakens the ceramic in the vicinity of the interface. This weakened zone is closely related to elaboration temperature (An *et al.* 2013). This temperature affects and controls the extent of the damaged zone due to the presence of residual stresses Hattali (2009). This extent is more important when Bi-materials is elaborated at high temperatures Hattali *et al.* (2009b).

## 2.2 Numerical prediction of the weakened (damaged) zone size of the ceramic

### 2.2.1 Geometrical model

A three-dimensional finite element method is conducted to model the ceramic-metal assembly, containing a central crack of length “a”. The crack is initiated in alumina bonded to silver, and is in parallel direction to the interface (see Fig. 12). ABAQUS software Karlson and Sorensen (2007) was used to predict and calculate the extent of the damaged zone in the ceramics under residual stresses effect. This extent will be analyzed in terms of variations of stress intensity factors (case of elastic behavior) and also in terms of the J integral (case of elastic-plastic behaviour). For this purpose, a geometric model, consisting of alumina perfectly bonded to silver, is subjected to different temperatures (see Fig. 12). These two materials are characterized, in elastic behavior, by their Young’s modulus and their respective Poisson coefficients:  $E_c = 320$  GPa,  $\nu_c = 0.27$  and  $E_m = 76$  GPa,  $\nu_m = 0.33$ . Alumina presents at these temperatures a linear elastic behaviour until failure while the metal has elastic-plastic behaviour (see Fig. 14).

Hexagonal quadratic elements of type C3D20R were employed. The overall mesh size includes 190820 elements and 811556 nodes. To ensure numerical accuracy, the mesh was refined near the contact region. The singularity at the crack tip was modeled using a specific refined mesh size (see Fig. 14). A convergence test was performed to obtain the adequate mesh size and to ensure the

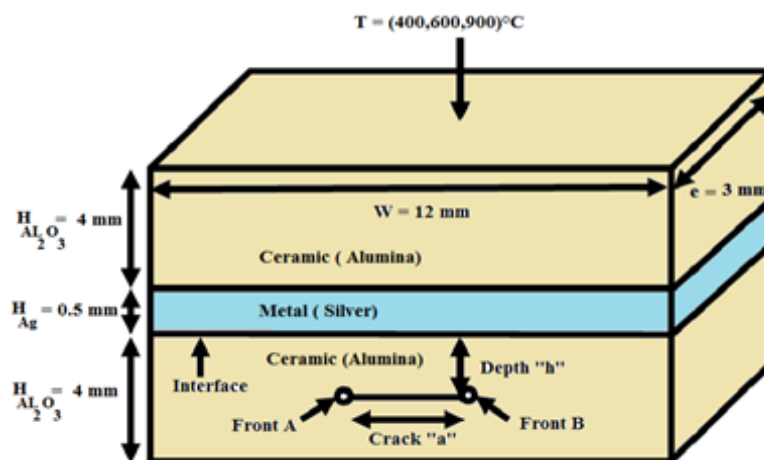


Fig. 12 Geometrical model

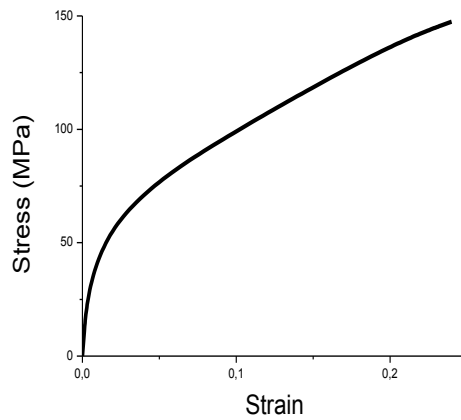


Fig. 13 True stress vs. strain curve of pure silver Wu and Lee (2016)

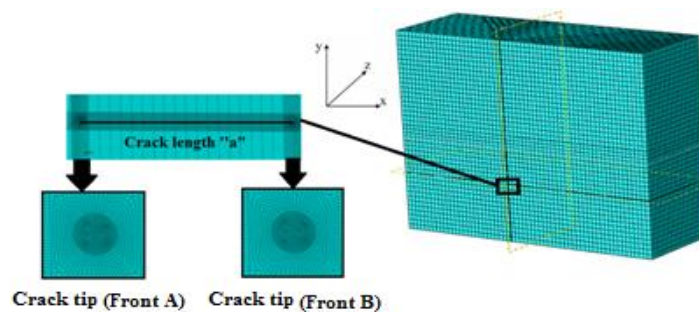


Fig. 14 Mesh size of the model studied

accuracy of the model. The integral  $J$  along the crack front in ABAQUS is implemented using the integral formulation of the domain Li *et al.* (1985). This procedure is similar to the virtual crack extension methods Shih *et al.* (1986). The  $J$  integral can be evaluated by integrating the field, determined from an elastic finite element analysis, along any contour lying within the crack tip region. The  $J$  integral is defined by

$$J = \int_{\Gamma} (w \cdot \delta_{1j} - \sigma_{ij} \cdot \frac{\delta u_i}{\delta x_1}) n_j d\Gamma \quad (5)$$

Here,  $\Gamma$  is a contour beginning at the crack bottom face and ending on the top face and  $n_j$  is the outward normal to  $\Gamma$ .  $w$  is the strain energy density computed by following the actual strain history for a linear elastic solid, and it depends only on the final strain,  $\sigma_{ij}$  represents stress components,  $u_j$  denotes the displacement.

### 2.2.2 Analysis of the damaged zone

In this part, a three-dimensional finite element analysis is carried out to predict the size of the weakened alumina zone, bonded to silver observed at 900°C, and experimentally determined by scanning electron microscopy (see Fig. 6(a)). To do this, the alumina-silver interface is considered

to be perfectly rigid in accordance with experimental results which showed that the cohesive fracture occurs in alumina (see Fig. 6(b)). Thus, a crack of length "a" is initiated in the alumina, in parallel direction to the interface, and in the vicinity of metal. We choose to put the crack in the ceramic material, because it's contains micro-cracks and defeats and therefore it is more likely that cracking occurs in ceramics rather than in metal (Table I). The extent of this zone is analyzed in crack tips A and B in terms of variation of stress intensity factors (elastic behaviour), and in terms of variation of the integral J (elastic-plastic behaviour). This variation is studied as a function of the bonding temperature, crack location, and its length. As mentioned earlier, this temperature generates residual compressive stresses in the ceramic, which are the principal cause of crack propagation.

In elastic behaviour, Figs. 15(a)-(b) and (c) clearly illustrate that in modes I, II and III, the cracking fronts A and B are less stable when the ceramic is bonded to the metal at high temperatures, and they propagate mainly in mixed modes. The mixed mode I and III are the predominant propagation mode (see Figs. 15(a) and (c)). Tangential residual interfacial stresses resulting from silver tension stresses and alumina compression stresses are responsible for the shear mode. This instability, described by a significant increase in the stress intensity factor and the elastic J integral, is more important for high crack length. In the opening mode, the cracking resistance of alumina, is affected when it is bonded to silver at too high temperatures (900°C) which is close to the melting point of the metal, regardless of the size of the cracking defect (see Fig. 15(a)). Fig. 16 shows that the residual stresses contribute considerably to mixed modes propagation of a crack initiated in the ceramic near to the interface.

Fig. 16 illustrates the effect of the elaboration temperature of alumina-silver assemblies on the integral J. It should be noted, that this fracture energy is very high when the materials are bonded at temperatures close to the melting point of the metal (900°C). Cracks initiated in the ceramic are less stable when the bonds are elaborated at such temperatures. This physical parameter generates stresses that can lead to damage the ceramic-metal assemblies.

To highlight the size of the weakened zone of alumina-silver assembly, the crack of length "a", initially initiated in the ceramic near the interface, was gradually moved away from this interface in the ceramic, at a depth "h", (see Fig. 12). In elastic behaviour, the propagation of this crack is analyzed in terms of variation of the stress intensity factors "SIF" in modes I, II and III and the integral J (see Figs. 17(a)-(b)-(c) and 18), at the cracking fronts noted here A and B, along this depth. Thus, these failure parameters are more significant as the crack is initiated in alumina near the silver interface, then they gradually decrease as it moves away from this zone. The results of

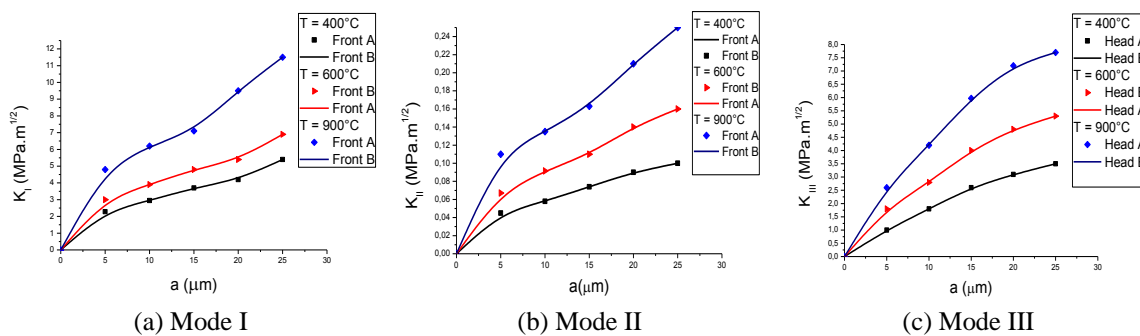


Fig. 15 Variation of the stress intensity factor with the crack size for different temperatures

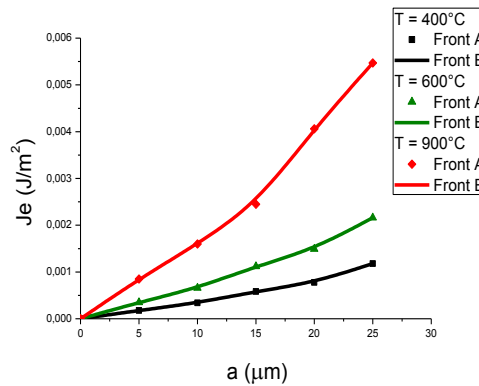


Fig. 16 Variation of the J-integral with the crack size for different temperatures (elastic approach)

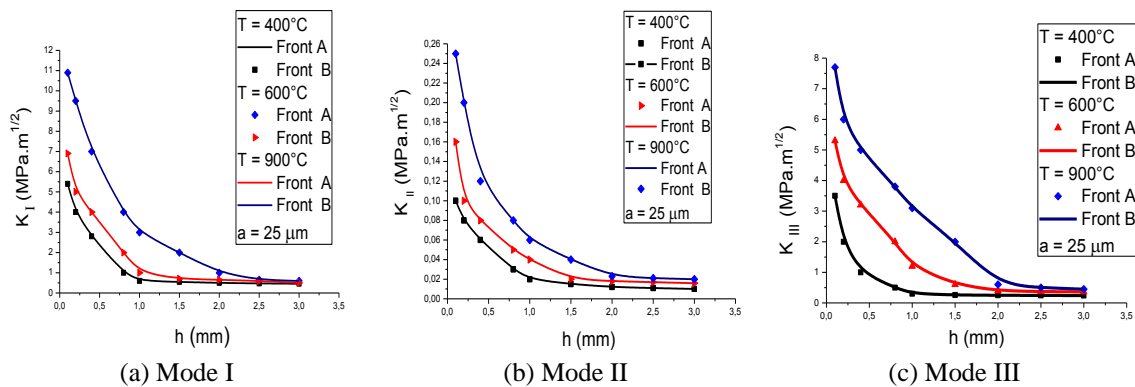


Fig. 17 Variation of the stress intensity factor, with the distance “h” for different temperature

this analysis show that the elaboration temperature controls the size of the crack instability zone (see Figs. 17(a)-(b)-(c) and 18). This zone is more extended when the ceramic is bonded to the metal at high temperatures, regardless of the propagation mode of the crack. Far from the interface, for an alumina bonded to this metal at a temperature of 900°C, which is the optimal temperature observed experimentally, this zone extends over a depth of about 2.5 mm. At this size, these propagation energies fall very significantly and take almost zero values. This depth, corresponding to the size of the weakened zone, is reduced as alumina is bonded to silver at low temperatures. It should be noted, however, that in elastic behaviour, this size obtained numerically is about three times more important than that obtained experimentally at the same temperature (see Fig. 6(a)). This behaviour clearly shows that at such a distance, the alumina is totally relaxed from the residual stresses and the interaction effect with the metal disappears completely. In this case, alumina behaves as a perfectly homogeneous material. The residual stresses, due to the elaboration of the bonds and highly concentrated in the close vicinity of the interface, are responsible for the evolution of these failure parameters. Residual stresses at the interface, tension in silver and compression in alumina, are responsible for such propagation in modes I and II. This behavior is in good coherence with that obtained by other studies (Guipont 1994 and Chama *et al.* 2014).

The elastic approach is not suitable for the analysis and the prediction of the weakened zone extent, because it leads to erroneous results.

Alumina is a brittle material whose mechanical behaviour is linear elastic until BDT. This is not the case for silver, which behaves plastically at relatively low stresses (see Fig. 13). In this part of the work, the elastic-plastic behaviour (see Fig. 19) of this metal is taken into consideration for the numerical prediction of the weakened zone size of alumina-silver bond. In the same way as in the elastic analysis, the crack, previously initiated in alumina and very close to the silver interface, was gradually moved away from this interface in alumina by a depth “h” (see Fig. 12). The extent of this zone is evaluated in terms of variation of the integral J (elastic and plastic) along this depth “h” (see Fig. 19). The analysis of this figure clearly illustrates that, compared to elastic behaviour, the plasticity of the metal lead to significantly lower values of the integral J and lower alumina damage depths, regardless of the crack initiation location in the alumina. Thus, the depth of the weakened alumina zone, about 0.70 mm, bonded to silver at a temperature of 900°C, observed experimentally, is in very good agreement with that estimated numerically at the same temperature whose value is about 0.80 mm (see Fig. 20). This value decreases when alumina is bonded to silver at low temperatures. The plastic deformation of silver bonded to alumina is essentially responsible for the lower values of the fracture energies numerically calculated (see Fig. 21). This

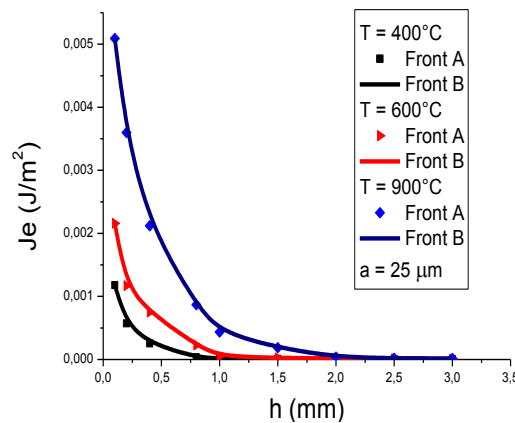


Fig. 18 Variation of the integral J with the distance “h” for different temperature (Elastic approach)

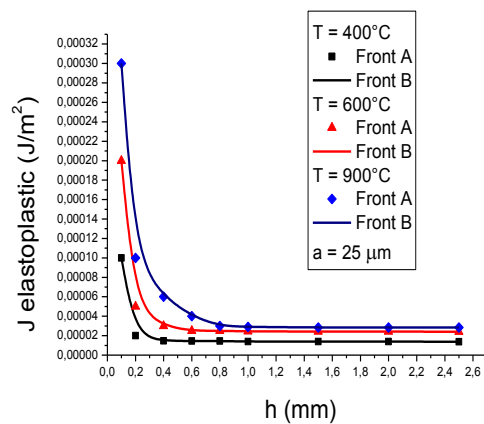


Fig. 19 Variation of the J integral with the distance “h” for different temperature (elastic-plastic approach)

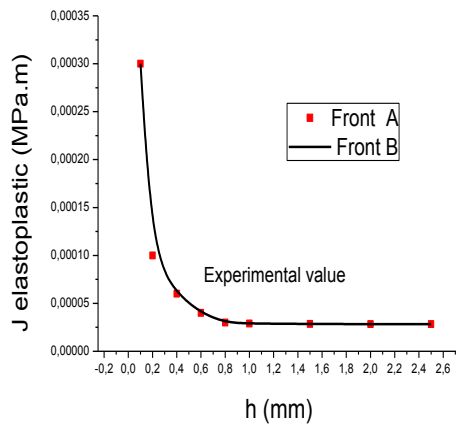


Fig. 20 Comparative analysis of the damaged zone depth “h” of alumina, assembled with silver at (T = 900°C), obtained numerically and experimentally

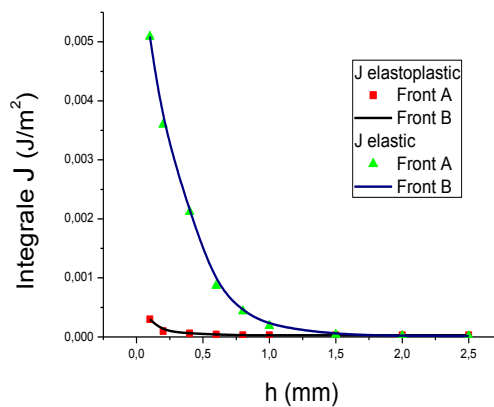


Fig. 21 Comparative analysis of the J integral in elastic and elastic-plastic with. the distance “h” (T = 900°C)

is in good agreement with the results obtained by Hway and Evans (2006). Indeed, the residual stresses strongly located near the interface are relaxed by the plasticization of silver. This decline in crack tip stresses is highly insufficient to lead to instability of the cracking fronts noted A and B.

This phenomenon leads to a considerable drop in these stresses and therefore a significant reduction of the damaged zone size in the ceramic.

This study explicitly shows that the three-dimensional numerical simulation, using the finite element method is able to predict the size of the weakened zone of the ceramic joined to a metal by solid state bonding, at a temperature close to the melting point of this metal. In fact, a very good correlation was illustrated between the extent (size) of this zone observed experimentally and that resulting from numerical modeling. This prediction highlights and describes the ceramic zone, which is in a strong interaction with the metal and severely weakened by thermal residual stresses. It was explained also how these stresses are responsible for reducing the lifecycle of this kind of assemblies. Indeed, this zone of ceramic is subjected to brittle fracture and therefore to early failure phenomena.

### 3. Conclusions

In the present study, a three-dimensional Finite Element Model has been developed to estimate the size of the weakened zone in the bi-materials a ceramic bonded to a metal. The calculations results were compared to those obtained using Scanning Electron Microscope (SEM). In the case of elastic-plastic behaviour, it has been shown that the simulation results are coherent with the experimental findings. This indicates that Finite Element modeling allows an accurate prediction and estimation of the weakening effect of residual stresses on the bonding interface of Alumina. The obtained results also enable us to deduce the three-dimensional numerical simulation using by the Finite Element Method allows a good prediction of the weakened zone extent of a ceramic which is in very strong interaction with a metal.

### References

- An, X.M., Zhao, Z.Y., Zhang, H.H. and He, L. (2013), "Modeling bimaterial interface cracks using the numerical manifold method", *Eng. Anal. Boundary Elem.*, **37**(2), 464-474.  
<https://doi.org/10.1016/j.enganabound.2012.11.014>
- Bešević, M. (2012), "Experimental investigation of residual stresses in cold formed steel sections", *Steel Compos. Struct., Int. J.*, **12**(6), 465-489. <https://doi.org/10.12989/scs.2012.12.6.465>
- Boutabout, B., Chama, M., Bachir, B.B., Serier, B. and Lousdad, A. (2009), "Effect of thermomechanical loads on the propagation of crack near the interface brittle/ductile", *Computat. Mater. Sci.*, **46**(4), 906-911.  
<https://doi.org/10.1016/j.commatsci.2009.04.039>
- Cazajus, V., Seguy, S., Weleman, H. and Karama, M. (2012), "Residual stresses in a ceramic-metal composite", *Appl. Mech. Mater.*, **146**, 185-196.
- Chama, M., Boutabout, B., Lousdad, A., Bensmain, W. and Bouiadjra, B.A.B. (2014), "Crack propagation and deviation in bi-materials under thermo-mechanical loading", *Struct. Eng. Mech., Int. J.*, **50**(4), 441-457. <https://doi.org/10.12989/sem.2014.50.4.441>
- Charles, Y., Hild, F., Duval, J. and Roux, S. (2005), "Analyse d'un mode de vieillissement dans un assemblage ceramique/metal", *Mécanique & Industries*, **6**(1), 101-115.  
<https://doi.org/10.1051/meca:2005011>
- Datta, D., Tomar, V. and Varma, A.H. (2018), "A path independent energy integral approach for analytical fracture strength of steel-concrete structures with an account of interface effects", *Eng. Fract. Mech.*, **204**, 246-267. <https://doi.org/10.1016/j.engfracmech.2018.10.011>
- Doitrand, A. and Leguillon, D. (2018), "3D application of the coupled criterion to crack initiation prediction in epoxy/aluminum specimens under four point bending", *Int. J. Solids Struct.*, **143**(15), 175-182.  
<https://doi.org/10.1016/j.ijsolstr.2018.03.005>
- England, A.H. (1965), "A crack between dissimilar media", *J. Appl. Mech.*, **32**, 400-402.  
<https://doi.org/10.1115/1.3625813>
- Erdogan, F. and Biricikoglu, V. (1973), "Two bonded half planes with a crack going through the interface", *Int. J. Eng. Sci.*, **11**(7), 745-766. [https://doi.org/10.1016/0020-7225\(73\)90004-9](https://doi.org/10.1016/0020-7225(73)90004-9)
- Guipont, V. (1994), "Déterminations expérimentales de contraintes résiduelles au sein d'assemblages céramique-métal réalisés par brassage : application au couple nitrure silicium-acier doux", Thèse de doctorat, Ecole Centrale de Lyon.
- Hattali, M.L. (2009), "Caracterisation et modelisation thermomécanique des assemblages Metal-Ceramique élaborés par thermocompression", Thèse de doctorat, Ecole Centrale de Lyon.
- Hattali, M.L., Valette, S., Ropital, F., Stremmsdoerfer, G., Mesrati, N. and Tréheux, D. (2009a), "Study of SiC-nickel alloy bonding for high temperature applications", *J. Eur. Ceramic Soc.*, **29**(4), 813-819.  
<https://doi.org/10.1016/j.jeurceramsoc.2008.06.035>

- Hattali, M.L., Valette, S., Ropital, F., Mesrati, N. and Tréheux, D. (2009b), "Effect of thermal residual stresses on the strength for both alumina/Ni/alumina and alumina/Ni/nickel alloy biomaterials", *J. Mater. Sci.*, **44**, 3198-3210. <https://doi.org/10.1007/s10853-009-3426-7>
- Haussonne, J.M., Carry, C., Bowen, P. and Barton, J. (2005), "Ceramique Et Verres : Principales Et Techniques D'élaboration", Lausanne : Presses polytechniques et universitaires Romandes, Paris, **6**, 446.
- Hu, X.F., Shen, Q.S., Wang, J.N., Yao, W.A. and Yang, S.T. (2017), "A novel size independent symplectic analytical singular element for inclined crack terminating at bimaterial interface", *Appl. Mathe. Model.*, **50**, 361-379. <https://doi.org/10.1016/j.apm.2017.05.046>
- Hutchinson, J.W. and Suo, Z. (1991), "Mixed mode cracking in layered materials", *Adv. Appl. Mech.*, **29**, 63-191.
- Hwang, I.H., Heoung, J.Ch., Hong, I.P., Yong, B.P. and Yoon, J.K. (2015), "Change of transmission characteristics of FSSs in hybrid composites due to residual stresses", *Steel Compos. Struct., Int. J.*, **19**(6), 1501-1510. <https://doi.org/10.12989/scs.2015.19.6.1501>
- Hsueh, C.H. and Evans, A.G. (2006), "Residual stresses in meta/ceramic bonded strips", *J. Am. Ceramic Soc.*, **68**(5), 241-248. <https://doi.org/10.1111/j.1151-2916.1985.tb15316.x>
- Itou, S. (2007), "Stress intensity factors for an interface crack between an epoxy and aluminium composite plate", *Struct. Eng. Mech., Int. J.*, **26**(1), 99-109. <https://doi.org/10.12989/sem.2007.26.1.099>
- Jarzabek, D.M. (2018), "The impact of weak interfacial bonding strength on mechanical properties of metal matrix-ceramic reinforced composites", *Compos. Struct.*, **201**, 352-362. <https://doi.org/10.1016/j.compstruct.2018.06.071>
- Jarzabek, D.M., Chmielewski, M., Dulnik, J. and Strojny-Nedza, A. (2016), "The influence of the particle size on the adhesion between ceramic particles and metal matrix in MMC composites", *J. Mater. Eng. Perform.*, **25**(8), 3139-3145. <https://doi.org/10.1007/s11665-016-2107-3>
- Karlsen & Sorensen (2007), ABAQUS Standard Version 6.9 User's manual, Inc., Hibbitt.
- Li, F.Z., Shih, C.F. and Needleman, A. (1985), "A comparison of methods for calculating energy release rate", *Eng. Fract. Mech.*, **21**(2), 405-421. [https://doi.org/10.1016/0013-7944\(85\)90029-3](https://doi.org/10.1016/0013-7944(85)90029-3)
- Liang, K.M., Orange, G. and Fantozzi, G. (1990), "Evaluation by indentation of fracture toughness of ceramic materials", *J. Mater. Sci.*, **25**(1), 207-214. <https://doi.org/10.1007/BF00544209>
- Liu, Z., Chen, X., Yu, D. and Wang, X. (2017), "Analysis of semi-elliptical surface cracks in the interface of bimaterial plates under tension and bending", *Theor. Appl. Fract. Mech.*, **93**, 155-169. <https://doi.org/10.1016/j.tafmec.2017.07.019>
- Ma, L., He, R., Zhang, J. and Shaw, B. (2013), "A simple model for the study of the tolerance of interfacial crack under thermal load", *Acta Mech.*, **224**(7), 1571-1577. <https://doi.org/10.1007/s00707-013-0820-7>
- Ouinias, D., Bouiadjra, B.B., Serier, B. and Vin, J. (2008), "Influence of bimaterial interface on kinking behaviour of a crack growth emanating from notch", *Computat. Mater. Sci.*, **41**(4), 508-514. <https://doi.org/10.1016/j.commatsci.2007.05.010>
- Rice, J.R. (1988), "Elastic fracture mechanics concepts for interfacial cracks", *J. Appl. Mech.*, **55**(1), 98-103. <https://doi.org/10.1115/1.3173668>
- Serier, B., Bouiadjra, B.B., Belhouari, M. and Treheux, D. (2011), "Experimental analysis of the strength of silver-alumina junction elaborated at solid state bonding", *Mater. Des.*, **32**(7), 3750-3755. <https://doi.org/10.1016/j.matdes.2011.03.047>
- Shih, C.F., Moran, B. and Nakamura, T. (1986), "Energy release rate along a three dimensional crack front in a thermally stressed body", *Int. J. Fract.*, **30**(2), 79-102. <https://doi.org/10.1007/BF00034019>
- Sih, G.C. and Rice, J.R. (1965), "Discussion of the bending of plates of dissimilar materials with cracks", *J. Appl. Mech.*, **32**(2), 464-466.
- Wu, J. and Lee, C.C. (2016), "The growth and tensile deformation behavior of the silver solid solution phase with zinc", *Mater. Sci. Eng.: A*, **668**, 160-165. <https://doi.org/10.1016/j.msea.2016.05.061>
- Xu, C., Qin, T., Yuan, L. and Noda, N.A. (2008), "Variations of the stress intensity factors for a planar crack parallel to a bimaterial interface", *Struct. Eng. Mech., Int. J.*, **30**(3), 317-330. <https://doi.org/10.12989/sem.2008.30.3.317>
- Zhang, H. and Qiao, P. (2017), "An extended state-based peridynamic model for damage growth prediction



of bimaterial structures under thermomechanical loading”, *Eng. Fract. Mech.*, **189**, 81-97.  
<https://doi.org/10.1016/j.engfracmech.2017.09.023>

CC